Contribution of Long-Range Electrostatic Interactions to the Stabilization of the Catalytic Transition State of the Serine Protease Subtilisin BPN′

Sophie E. Jackson[‡,§] and Alan R. Fersht[*]

M.R.C. Unit for Protein Function and Design, Cambridge I.R.C. for Protein Engineering, University Chemical Laboratory, Lensfield Road, Cambridge CB2 1EW, U.K.

Received June 30, 1993; Revised Manuscript Received October 5, 1993[●]

ABSTRACT: The possible role of long-range electrostatic interactions on the catalytic activity of the serine protease subtilisin BPN′ is investigated using protein engineering techniques. Charged residues on the surface of the enzyme some 13–15 Å from the active site were mutated to either neutral or oppositely charged residues. The effect of these mutations on the stability of a complex formed between subtilisin BPN′ and Z-Ala-Ala-Pro-Phe-trifluoromethyl ketone, a transition-state inhibitor of the enzyme, was measured. The values of K_i for the complex between the trifluoromethyl ketone and wild-type and mutant subtilisins were used to study the possible contribution of long-range electrostatics in stabilizing the charge distribution in the complex and thus, by analogy, on the transition state of hydrolysis for subtilisin BPN′. Measurement of k_{on}, k_{off}, and K_i for the inhibition of wild-type and mutant subtilisins showed that charged mutations distant from the active site can affect k_{off} and K_i but have little effect on k_{on}. The experimental results show that there is a small, 0.10–0.46 kcal mol^{-1}, but significant contribution to the binding energy from distant surface charges, at low ionic strength. The experimental results were compared to theoretical results, calculated using the DelPhi program for different charge distributions in the complex. The experimental results were found to be most consistent with a complex in which an ion pair is formed between the protonated active site histidine and the ionized oxyanion. Both experimental and theoretical results suggest that long-range electrostatic interactions do play a role in stabilizing the transition-state complex formed between enzyme and inhibitor. Although these effects are small, this suggests that long-range electrostatic interactions also play a role in stabilizing catalytic transition states. This maybe particularly important in enzymes which have a very asymmetric distribution of surface charge.

Electrostatic effects are of considerable importance in enzyme catalysis and are thought to play a major part in stabilizing charged transition states (Perutz, 1978; Matthew et al., 1979; Warshel, 1981; Warshel et al., 1984). In addition, the pH dependence of enzyme catalysis frequently depends on the ionization of catalytic groups, the pK_as of which are sensitive to their electrostatic environment. Understanding the role of electrostatics in proteins is, therefore, of fundamental importance for understanding enzyme catalysis.

Long-range electrostatic interactions have now been shown to be important in a number of biological processes, including molecular recognition and binding (Koppenol, 1981; Koppenol & Margoliash, 1982; Northrup et al., 1988), folding (Tweedy et al., 1990; Perry et al., 1989), and determining the pK_as of ionizable residues such as histidines (Thomas et al., 1985; Russell & Fersht, 1987; Russell et al., 1987; Cederholm et al., 1991; Loewenthal et al., 1993). Despite these studies there is still no direct evidence that long-range electrostatic interactions also affect the transition state of an enzyme and its catalytic activity.

Recently, some theoretical studies have tried to predict the effect of surface charge on the catalytic activity of a number of enzymes. Calculations carried out by Honig and co-workers have predicted negligible effects of surface charges on the catalytic activity of trypsin isozymes (Soman et al., 1989), while other studies, on actinidin and papain, have indicated that surface charge, as well as specific active site residues, can play an important role in catalysis (Pickersgill et al., 1988). The results from calculations on lysozyme (Dao-Pin et al., 1989) and triosephosphate isomerase (Bash et al., 1991) also suggest that distant electrostatic interactions may contribute to the activity of these enzymes.

In this study we take an experimental approach to the problem. The possible role of long-range electrostatic interactions on the catalytic activity of the serine protease subtilisin BPN′ from *Bacillus amyloliquefaciens*, is investigated using protein engineering techniques.

Subtilisins catalyze the hydrolysis of peptide and ester bonds. In subtilisin BPN′, the catalytic triad consists of residues His64, Ser221, and Asp32. His64 acts as general base during catalysis, accepting a proton from Ser221 as it forms a bond with the substrate carbonyl carbon. In the resulting tetrahedral transition state the histidine is believed to be protonated and the oxyanion ionized. The ion pair is stabilized by Coulombic interactions between the two. The protonated histidine is stabilized further by Coulombic interactions with the active site aspartic acid, and the oxyanion by hydrogen bonds from the backbone amide of Ser221 and from the amide side chain of Asn155 (Bryan et al., 1986). The tetrahedral transition state collapses to form an acylenzyme which then undergoes a rapid deacylation. Catalysis is achieved by the specific binding and stabilization of the tetrahedral transition state characteristic of acyl-transfer mechanisms (Robertus et al., 1972). In this paper we look at how long-range electrostatic interactions can stabilize this charged tetrahedral transition state.

k_{cat} and k_{cat}/K_m are both measures of the stabilization of the catalytic transition state of an enzyme. However, while the pK_a of the active site histidine can be measured within an

* Author to whom correspondence should be addressed.
‡ Present address: Department of Chemistry, Harvard University, 12 Oxford St., Cambridge, MA 02138.
§ S.E.J. was supported by a SERC studentship.
● Abstract published in *Advance ACS Abstracts*, November 15, 1993.

0006-2960/93/0432-13909$04.00/0

accuracy of ±0.01 pH units, k_{cat} cannot be measured to the same degree of accuracy because the value is dependent on the absolute concentration of enzyme. Subtilisins are known to autolyse, and, despite an active-site titration for the enzyme (Bender et al., 1966), the errors involved in measuring k_{cat} are still significant. This study circumvents these problems by using a transition-state inhibitor of the enzyme and measuring K_i, which, unlike k_{cat}, can be measured directly without the need to know the absolute concentration of the enzyme. Thus, the effects of long-range electrostatic interactions on the catalytic transition state of the enzyme can be inferred from the experimentally determined effects of long-range electrostatic interactions on the stability of the complex formed between subtilisin BPN′ and the transition-state inhibitor. The transition state inhibitor used in these studies is a peptidyl trifluoromethyl ketone.

There is now a great deal of evidence that not only shows that peptidyl trifluoromethyl ketones are reversible inhibitors of many serine proteases (Imperiali & Abeles, 1986, 1987; Liang & Abeles, 1987; Brady et al., 1989; McMurray & Dyckes, 1986; Angliker et al., 1988; Stein et al., 1987; Dunlap et al., 1987; Takahashi et al., 1989; Govordham & Abeles, 1990) but that they are transition state inhibitors of such enzymes (Takahashi et al., 1988; Imperiali & Abeles, 1986; Allen & Abeles, 1989; Stein et al., 1987; Brady et al., 1989). By analogy with these results we assume that the peptidyl trifluoromethyl ketone forms a covalent complex with subtilisin BPN′ analogous to the transition state for amide hydrolysis. Attack of the active site serine Oγ on the carbonyl carbon of the inhibitor and transfer of a proton from the hydroxyl group of the serine residue to the active site histidine leads to the formation of a tetrahedral hemiketal moiety which resembles the tetrahedral transition state in the normal catalytic process.

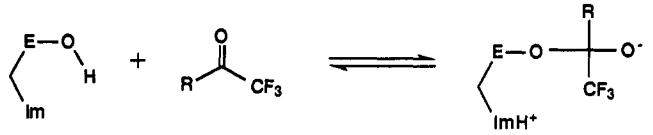

Charged residues some 13–15 Å from the active site, which are on the surface of the enzyme and which are not directly involved in either substrate binding or in the catalytic mechanism, were mutated to either neutral or oppositely charged residues. Thus, we can probe both the charge distribution in the transition state for hydrolysis for subtilisin BPN′ and the effect of long-range electrostatic interactions on this charge distribution, by measuring the effect of these charge mutations on the complex formed between subtilisin BPN′ and the peptidyl trifluoromethyl ketone inhibitor.

We also compare the results obtained experimentally to those calculated using the finite difference method (Warwicker & Watson, 1982) of calculating electrostatic interactions using the DelPhi[1] software package.

EXPERIMENTAL PROCEDURES

Materials

Chemicals. Z-Ala-Ala-Pro-Phe-trifluoromethyl ketone was a generous gift from Robert H. Abeles. It was prepared as a stock solution in dry dimethyl sulfoxide (DMSO). DMSO used for stock substrate and inhibitor solutions was dried over barium oxide and distilled under vacuum. Water used in all experiments was purified to 15 MΩ resistance by an Elgastat system. All other chemicals were purchased from Sigma. Wild-type and mutant subtilisin BPN′ were prepared, expressed, and purified as described elsewhere (Thomas et al., 1985; Russell & Fersht, 1987; Russell et al., 1987). The final purified protein was flash frozen and stored at −70 °C.

Methods

Determination of K_m for the Hydrolysis of Succinylalanylalanylprolylphenylalanyl-p-nitroalanine. Stock solutions of the substrate succinylalanylalanylprolylphenylalanyl-*p*-nitroalanine (sAAPFpNA) were prepared in low, medium, and high ionic strength buffers. The low ionic strength buffer was 10 mM Tris-HCl, pH 8.6, 0.05% Tween, the medium ionic strength buffer was 0.1 M Tris-HCl, pH 8.6, 0.05% Tween, and the high ionic strength buffer was 0.1 M Tris-HCl, pH 8.6, 1 M NaCl, 0.05% Tween. All the buffers were prepared from a stock of 1.0 M Tris-HCl, pH 8.6, which was frozen in aliquots, stored at −20 °C, and thawed when required. These stock solutions of substrate were then diluted as necessary, substrate concentrations varying between 0.2- and 5-fold K_m. The substrate concentrations were calculated from the final absorbance at 412 nm based on E_{412} = 8480 M^{-1} cm^{-1} (DelMar et al., 1979). The reaction was initiated by the addition of 10 μL of enzyme (approximately 5 μM enzyme in 10 mM MES, pH 6.2, 2 mM $CaCl_2$, 0.05% Tween) to 1 mL of buffered substrate in a cuvette thermostated at 25 °C, in a Perkin-Elmer λ5 spectrophotometer. Enzyme concentrations were determined spectrophotometrically using an extinction coefficient of 3.22 × 10^4 M^{-1} cm^{-1} at 280 nm (Matsubara et al., 1965). Tween (0.05%) was added to both enzyme and substrate solutions to reduce the loss of enzyme activity due to adsorption of the enzyme on the walls of the cuvettes. Initial rates were calculated from the increase in absorbance at 412 nm from the release of *p*-nitroaniline using E_{412} = 8480 M^{-1} cm^{-1} (DelMar et al., 1979). Initial rates were measured at 10–20 substrate concentrations, and the data were fitted to the Michaelis–Menten equation using the nonlinear regression program Enzfitter (Elsevier Biosoft, Cambridge, MA) by R. J. Leatherbarrow.

Slow-Binding Inhibition Kinetics. Inhibitors are treated as slow binding when the attainment of a steady-state enzyme activity can be observed over a time period of several minutes, and data can be successfully fitted to the slow-binding eq 1 [see Williams and Morrison (1979) and Cha (1975) for reviews]. For the simplest treatment of slow-binding data, experiments were carried out under pseudo-first-order conditions, where the lowest [I] ≥ 10[E]. The enzyme concentration was typically 5 pM; this gives a measurable rate of substrate hydrolysis as well as an observable rate of inhibitor binding over the steady-state time scale. The range of inhibitor concentrations used depended on the dissociation constant for the complex and varied with ionic strength. Inhibitor concentrations varied between 2.5 and 15 μM for experiments at low and medium ionic strengths and between 1 and 3 μM for the high salt experiment. The inhibitor was stored as a stock solution (0.6 mM) in dry DMSO at −20 °C. The substrate solution was made from a stock (50 mM) of sAAPFpNA in DMSO. The initial concentration of substrate was sufficiently high to allow the reaction to be followed for an adequate time for data collection but with less than 10% of substrate being hydrolyzed by the end of the experiment. The substrate concentration was determined from the final absorbance as described above and was typically 0.3–0.4 mM. Six cuvettes (3 mL) containing substrate and inhibitor were incubated at 25 °C in a Perkin-Elmer λ5 double-beam spectrophotometer fitted with an automatic cell changer (2 × six cells). Six cuvettes containing 3 mL of buffered substrate were used as blanks. Reactions were initiated by the addition

[1] DelPhi version 2.3, Biosym Technologies, San Diego, CA.

of 10 μL of enzyme solution. Data were collected using the PECSS package provided by Perkin-Elmer for 5–6 h. The data were translated into ASCII format using the J-camp facility within the PECSS program and then analyzed using the nonlinear regression program Enzfitter, as described below.

Data Analysis. Data from each curve at different inhibitor concentrations were fitted to eq 1, the integrated rate equation describing substrate hydrolysis in the presence of slow-binding inhibitor (Williams & Morrison, 1979; Cha, 1975).

$$A = v_s t + (v_o - v_s)[1 - \exp(-k_{obs}t)]/k_{obs} + A_o \quad (1)$$

where A is the absorbance at 412 nm, A_o is the initial absorbance, v_o is the initial rate, v_s is the final steady-state rate, and k_{obs} is the apparent first-order rate constant for the transition to the steady-state rate. Curve fitting gives values for the four independent variables, v_o, v_s, k, and A_o, at each concentration of inhibitor. For the simplest model of complex formation,

$$E + I \underset{k_{off}}{\overset{k_{on}}{\rightleftharpoons}} EI$$

a plot of k_{obs} versus [I] gives a straight line from which k_{on} and k_{off}, the association and dissociation rate constants; respectively, can be determined according to

$$k_{obs} = k_{off} + k_{on}[I]/(1 + [S]/K_m) \quad (2)$$

A plot of $(v_o - v_s)/v_s$ versus [I] can be used to determine K_i, the dissociation constant, and should give a straight line passing through the origin according to

$$(v_o - v_s)/v_s = [I]/[K_i(1 + [S]/K_m) \quad (3)$$

Where v_o cannot be determined accurately from fitting, eq 3 can still be used to calculate K_i, but the uninhibited enzyme rate is used instead of v_o.

Theoretical Calculations. The DelPhi software package calculates electrostatic potentials in and around macromolecules by solving the nonlinear Poisson Boltzmann equation by the finite difference method (Gilson & Honig, 1987; Gilson et al., 1988). This was used to calculate the interaction energies between the mutated surface charges, at positions 36 and 99, and the histidine and oxyanion in free and complexed subtilisin BPN′. A Silicon Graphics Indigo Computer was used to run the DelPhi program. Default settings in version 2.3 were used, the solvent dielectric constant = 80, and the solute dielectric constant = 2.0. No water molecules were explicitly included in the crystal structure since they would be assigned a dielectric constant of 2. One half of the electron charge was placed on each of the $N^{\delta 1}$ and $N^{\epsilon 2}$ positions of His64 and a single charge on the oxyanion.

Description of Mutations. (*i*) *Asp → Gln36.* Aspartic acid 36 is located in a surface loop outside the active site cleft. It is separated from His64 by protein, including the α-helix containing His64, by 15–16 Å. This residue was replaced by a glutamine.

(*i*) *Asp → Ser99*; *Asp → Lys99.* Aspartic acid 99 is in an external loop of the enzyme on the rim of the active site cleft about 12–13 Å away from His64. The environment between the Asp99 and His64 is mainly protein. This residue was replaced by a serine and a lysine.

Studies on the effect of these mutations on the ground state of the enzyme have shown that, at low ionic strength, the mutations destabilize the protonated form of the active site histidine leading to a downward shift in the pK_a of catalysis of some 0.1–0.2 pH units (Thomas et al., 1985; Russell & Fersht, 1987; Russell et al., 1987). This paper describes the effect of these mutations on the catalytic transition state of the enzyme.

Table I: K_m for the Hydrolysis of sAAPFpNA by Wild-Type and Mutant Subtilisins at Varying Ionic Strength

	k_{cat} (s^{-1})		K_m (mM)	
protein	i = 0.1 M[b]	i = 0.01 M[a]	i = 0.1 M[b]	i = 1.1 M[c]
wild-type	68 ± 14	0.106 ± 0.005	0.106 ± 0.003	0.096 ± 0.002
Asp → Ser99	54 ± 11	0.073 ± 0.004	0.077 ± 0.003	0.103 ± 0.002
Asp → Lys99	61 ± 12	0.077 ± 0.002	0.093 ± 0.003	0.128 ± 0.004
Asp → Gln36	78 ± 16	0.120 ± 0.008	0.107 ± 0.002	0.104 ± 0.003

[a] 10 mM Tris-HCl, pH 8.6, 0.05% Tween. [b] 100 mM Tris-HCl, pH 8.6, 0.05% Tween. [c] 100 mM Tris-HCl, pH 8.6, 1 M NaCl, 0.05% Tween.

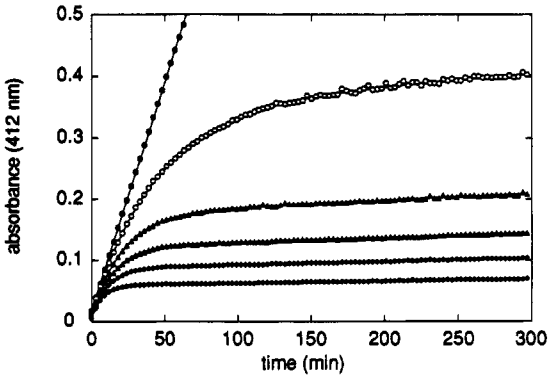

FIGURE 1: Typical family of slow, tight-binding curves for the inhibition of subtilisin BPN′ by zAAPF-trifluoromethyl ketone. Inhibitor concentrations were 0 μM (●), 2.5 μM (○), 5 μM (▲), 7.5 μM (△), 10 μM (♦), and 15 μM (◇) Z-Ala-Ala-Pro-Phe-trifluoromethyl ketone. The best fit of the data to eq 1 is shown by the solid lines.

RESULTS

Determination of K_m for the Hydrolysis of sAAPFpNA by Wild-Type and Mutant Subtilisin BPN′. The subtilisin-catalyzed hydrolysis of amide substrates shows Michaelis–Menten kinetics. The K_m for the hydrolysis of the substrate, sAAPFpNA, was determined for wild-type and mutant enzymes in 10 mM Tris-HCl, 100 mM Tris-HCl, and 100 mM Tris-HCl and 1 M NaCl, at pH 8.6 and 0.05% Tween. In all cases the data could be fitted to the Michaelis–Menten equation, and the Eadie–Hofstee plots were linear. The results are summarized in Table I. There are small variations in the value of K_m with mutation and ionic strength. These are the result of electrostatic interactions between the enzyme and the substrate, which is negatively charged under the experimental conditions. The values of K_m given in Table I are used in the calculation of k_{on} and K_i (see eqs 2 and 3).

Inhibition of Subtilisin BPN′ by a Peptidyl Trifluoromethyl Ketone. Wild-type and mutant subtilisins are all reversibly inhibited by the peptidyl trifluoromethyl ketone, zAAPF-TFMK, shown below.

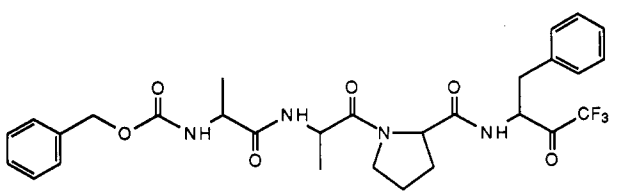

In all cases zAAPF-TFMK was found to be a slow-binding inhibitor; steady-state rates were achieved after some 5–6 h depending upon the inhibitor concentration. A typical set of binding curves is shown in Figure 1. Data from these

experiments were fitted to eq 1 to give values for k_{obs}, v_o, and v_s at each inhibitor concentration.

Association Rates. Plots of k_{obs}, obtained from the binding curves, versus inhibitor concentration were used to calculate the association rate, k_{on}, for the binding of the inhibitor to wild-type and mutant subtilisins. A typical plot of k_{obs} versus inhibitor concentration is shown in Figure 2A. For wild-type and mutants, these plots were linear over the inhibitor concentration range studied, at all ionic strengths studied. The kinetic data are thus consistent with a reaction in which enzyme and inhibitor combine to form the final complex, i.e., no Michaelis-like noncovalent intermediate is required.

$$E + I \underset{k_{off}}{\overset{k_{on}}{\rightleftharpoons}} EI$$

Evidence from other studies on transition-state inhibitors of serine proteases suggests a mechanism involving the initial formation of a noncovalent EI complex followed by a rate-limiting conformational change (Stein et al., 1987; Kettner & Shenvi, 1984; Stein & Strimpler, 1987). A similar mechanism for the inhibition of subtilisin BPN′ by the peptidyl trifluoromethyl ketone cannot be excluded, on the condition that the dissociation constant for the initial noncovalent complex is greater than approximately 0.6 μM.

The values for k_{on} shown in Table II are based on an inhibitor concentration calculated directly from a stock solution in DMSO. However, in aqueous solution, an equilibrium exists between the hydrated form and the keto form.

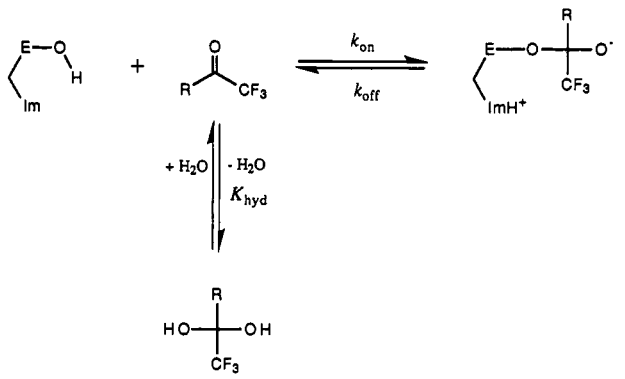

For trifluoromethyl ketones, the equilibrium lies well over toward hydrate formation. Studies on acetylcholinesterase have shown that only the keto form reacts with enzyme to form a stable complex (Allen & Abeles, 1989); therefore, the effective concentration of the inhibitor in solution is substantially less than that calculated. A corrected value for k_{on}, k_{on}(cor), can be calculated by taking into account the equilibrium due to hydration of the inhibitor.

$$k_{on}(cor) = k_{on}(1 + K_{hyd}) \quad (4)$$

K_{hyd}, the equilibrium constant for hydration, has been measured for various trifluoromethyl ketones. Values of 77 (Ritchie, 1984), 100 (Stein et al., 1987), 387 (Smith et al., 1988), and 500 (Allen & Abeles, 1989) have all been reported for various trifluoromethyl ketone derivatives. It is likely that the equilibrium constant for the hydration of zAAPF-TFMK lies within this range. This suggests that the real values for k_{on} are in the range (1–3) × 10^5 M^{-1} s^{-1}. These values are only 100–1000 less than diffusion-controlled limits and do not represent slow-binding. The origin of slow binding is, therefore, not a result of a small association constant, but the result of a very low effective concentration of inhibitor.

There is relatively little difference in the association rates between wild-type and mutant enzymes; however, the values

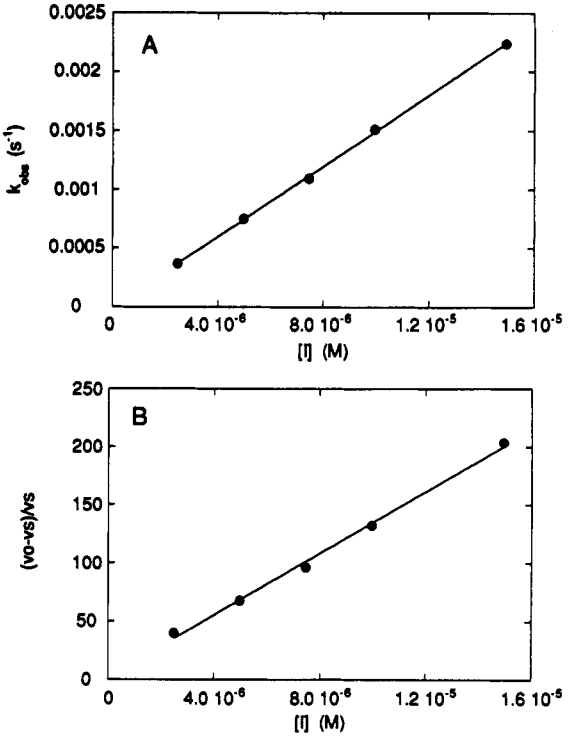

FIGURE 2: Typical plots for the determination of (A) k_{on} and (B) K_i from the slow, tight-binding curves. (A) Plot of k_{obs}, determined at each inhibitor concentration by fitting the data from Figure 1 to eq 1, versus inhibitor concentration. From the slope and intercept on the y axis, values for k_{on} and k_{off} can be determined, respectively. (B) Plot of $(v_o - v_s)/v_s$, also determined by fitting the data from Figure 1 to eq 1, versus inhibitor concentration. K_i can be determined from the slope of the plot.

at high ionic strength are almost 2-fold larger. This could either be due to an increase in k_{on} or a result of changes in the hydrate–ketone equilibrium, which would affect the effective concentration of inhibitor.

Dissociation Constants. K_i, the dissociation constant for the complex formed between enzyme and inhibitor, was determined from the values of v_o and v_s obtained from the best fit of the binding curves to eq 1. Figure 2B shows a typical plot of $(v_o - v_s)/v_s$ versus inhibitor concentration. This plot is linear and passes through the origin. For slow-binding inhibitors, equilibrium is reached slowly, and it is important to run the experiments for sufficient time so that a good estimate of v_s can be obtained from the fitting. In this case, experiments were run for 5–6 h. If the experiment is not run for sufficient time, then systematic errors can be generated that can be misinterpreted as unusual binding. This is readily diagnosed in plots such as those shown in Figure 2B, which become nonlinear in these cases. All the plots of $(v_o - v_s)/v_s$ versus inhibitor concentration were found to be linear. K_i was determined from the slope of such plots using eq 3. The results for wild-type and mutant enzymes are summarized in Table II.

The hydrate–ketone equilibrium also affects the dissociation constant. A corrected value for the dissociation constant, K_i(cor), can be calculated.

$$K_i(cor) = K_i/(1 + K_{hyd}) \quad (5)$$

Thus, the real dissociation constants are some 100–500-fold less than the measured values, lying somewhere in the range 1×10^{-11} and 6×10^{-10} M, i.e., the inhibitor binds very tightly to form an extremely stable complex. This complex is much more stable than expected for an enzyme bound hemiketal derived from a trifluoromethyl ketone (Stein et al., 1987) and reflects both the structural analogy of the complex with the

Table II: k_{on}, k_{off}, and K_i Determination for Wild-Type and Mutant Subtilisins with the Slow, Tight-Binding Inhibitor zAAPF-Trifluoromethyl Ketone

protein	k_{on} (M^{-1} s^{-1})			K_i ($\times 10^8$ M)			k_{off} ($\times 10^5$ s)		
	i = 0.01 M[a]	i = 0.1 M[b]	i = 1.1 M[c]	i = 0.01 M[a]	i = 0.1 M[b]	i = 1.1 M[c]	i = 0.01 M[a]	i = 0.1 M[b]	i = 1.1 M[c]
wild-type	502 ± 28	534 ± 24	1180 ± 54	2.66 ± 0.15	1.98 ± 0.09	0.76 ± 0.04	1.34 ± 0.11	1.06 ± 0.07	0.90 ± 0.07
Asp → Ser99	542 ± 33	497 ± 26	1310 ± 60	3.65 ± 0.23	2.80 ± 0.19	0.90 ± 0.09	1.87 ± 0.17	1.39 ± 0.12	1.18 ± 0.13
Asp → Lys99	551 ± 26	477 ± 21	1330 ± 61	5.79 ± 0.27	5.26 ± 0.23	1.32 ± 0.06	3.19 ± 0.21	2.51 ± 0.16	1.76 ± 0.11
Asp → Gln36	542 ± 35	533 ± 22	1250 ± 52	3.15 ± 0.22	2.78 ± 0.12	0.75 ± 0.06	1.71 ± 0.16	1.48 ± 0.09	0.94 ± 0.09

[a] 10 mM Tris-HCl, pH 8.6, 0.05% Tween. [b] 100 mM Tris-HCl, pH 8.6, 0.05% Tween. [c] 100 mM Tris-HCl, pH 8.6, 1 M NaCl, 0.05% Tween.

catalytic transition state and also the enzyme's ability to stabilize such a transition state. Such tight binding suggests that the inhibitor binds to subtilisin BPN′ as a transition-state analogue, consistent with the evidence found for other serine proteases (Imperiali & Abeles, 1986; Liang & Abeles, 1987; Stein et al., 1987; Takahashi et al., 1988; Allen & Abeles, 1989; Brady et al., 1989).

In comparison to the value of k_{on}, significant differences in K_i are observed between wild-type and mutant enzymes at all ionic strengths. A general trend is observed with K_i increasing, i.e., the enzyme–inhibitor complex is destabilized, with increasing positive charge on the surface of the enzyme. K_i decreases, i.e., the complex becomes more stable with increasing ionic strength. This is consistent with the hypothesis that long-range electrostatic interactions from charged residues at positions 36 and 99 can affect the stability of the charge distribution in the complex. The implications of these results for possible charge distributions in the complex are discussed in greater detail later.

Dissociation Rates. Theoretically, the dissociation rate, k_{off}, can be determined from the intercept on the y axis of a plot, such as that shown in Figure 2A. In this case, however, the intercept is so close to zero that an accurate value cannot be measured. In addition, an accurate value could not be determined directly from the dissociation kinetics because the stability of the complex is such that the half-life for dissociation is so slow that the reaction cannot be followed for sufficient time for a steady state to be achieved. Values for k_{off} were determined indirectly from measurements of k_{on} and K_i ($k_{off} = K_i k_{on}$). The results are summarized in Table II. The trends observed in K_i are also observed in k_{off}.

Calculation of $\Delta\Delta G_{binding}$, the Difference in the Free Energy of the Enzyme–Inhibitor Complex between Wild-Type and Mutant Enzymes. $\Delta\Delta G_{binding}$, the difference in the free energy of the enzyme–inhibitor complex between wild-type and mutant enzymes, can be calculated from the experimentally determined dissociation constants. Defining $\Delta\Delta G_{binding}$ as

$$\Delta\Delta G_{binding} = \Delta G_{wild\text{-}type} - \Delta G_{mutant} \quad (6)$$

with $\Delta G_{wild\text{-}type} = -RT \ln K_{i\ wild\text{-}type}$ and $\Delta G_{mutant} = -RT \ln K_{i\ mutant}$, it follows that

$$\Delta\Delta G_{binding} = RT \ln (K_{i\ mutant}/K_{i\ wild\text{-}type}) \quad (7)$$

The values of $\Delta\Delta G_{binding}$ calculated for the mutants are shown in Table III. All mutations, except Asp → Gln36 at high salt, result in a destabilization of the enzyme–inhibitor complex, i.e., $\Delta\Delta G_{binding}$ is positive.

Theoretical Calculation of the Electrostatic Contribution to the Binding Energy. In addition to the experimentally determined $\Delta\Delta G_{binding}$, which is based on measured dissociation constants, the electrostatic contribution to the binding energy, $\Delta\Delta G_{calc}$, can be calculated theoretically using the DelPhi program (Gilson & Honig, 1987; Gilson et al., 1988). We ran the DelPhi program on the structure of the free enzyme (Bott et al., 1988) in order to calculate the effect of the charges at positions 36 and 99 on the active site histidine in the ground state of the enzyme. For the mutations Asp → Gln36 and Asp → Ser99, the results can simply be taken from the calculation on the wild-type enzyme. For the mutation Asp → Lys99 the lysine residue had to be modeled into the structure. This was done using the computer graphics program FRODO (Jones, 1978). The lysine side chain was built in an extended conformation. The calculated values are shown in Table IV. In this case, there is a good agreement between the values measured experimentally (Thomas et al., 1985; Russell & Fersht, 1987; Russell et al., 1987; Loewenthal et al., 1993) and those calculated using the DelPhi program. In this case, the active site of the enzyme is solvated, and the calculation only considers the interaction between the surface charge and the active site histidine.

Table III: $\Delta\Delta G_{binding}$, the Difference in the Free Energy of the Enzyme–Inhibitor Complex between Wild-Type and Mutant Subtilisins at Varying Ionic Strength

mutant	$\Delta\Delta G_{binding}$ (kcal mol^{-1})		
	i = 0.01 M[a]	i = 0.1 M[b]	i = 1.1 M[c]
Asp → Ser99	0.15 ± 0.05	0.20 ± 0.05	0.10 ± 0.07
Asp → Lys99	0.46 ± 0.04	0.58 ± 0.04	0.32 ± 0.04
Asp → Gln36	0.10 ± 0.09	0.20 ± 0.04	−0.01 ± 0.06

[a] 10 mM Tris-HCl, pH 8.6, 0.05% Tween. [b] 100 mM Tris-HCl, pH 8.6, 0.05% Tween. [c] 100 mM Tris-HCl, pH 8.6, 1 M NaCl, 0.05% Tween.

In order to calculate the electrostatic contribution for the binding of the transition-state inhibitor to wild-type and mutant enzymes, one must also take into account (i) the interaction between the surface charge and the total charge distribution in the transition state, i.e., the active site histidine and the oxyanion, and (ii) the fact that when either substrate or inhibitor is bound the active site is no longer solvated. This was achieved by creating a model structure of the subtilisin trifluoromethyl ketone inhibitor complex, which was based on the known crystal structure of subtilisin BPN′ complexed to chymotrypsin inhibitor 2 (CI2) (McPhalen & James, 1985). The peptidyl trifluroromethyl ketone inhibitor was modeled into the structure using the coordinates of CI2. The position of the oxyanion was taken as the position of the oxygen of Met59 (reactive site residue) of the inhibitor. The Asp → Lys99 mutation was modeled in a way identical to that described for the free enzyme. The electrostatic interaction energies calculated between the charges on Asp99, Lys99, and Asp36 and the active site histidine, $\Delta\Delta G_{+/0}$, and the oxyanion, $\Delta\Delta G_{0/-}$, are given in Table V. In addition, an overall interaction energy, $\Delta\Delta G_{+/-}$, which is simply the sum of $\Delta\Delta G_{+/0}$ and $\Delta\Delta G_{0/-}$, is also given.

Increasing the positive charge on the surface of the enzyme destabilizes the positively charged protonated histidine and stabilizes the negatively charged oxyanion, i.e., the values for $\Delta\Delta G_{+/0}$ are positive and the values for $\Delta\Delta G_{0/-}$ are negative. Figure 3 shows the stereochemical relationship between the charges on Asp36, Asp99, and Lys99 and the possible charges in the complex between subtilisin BPN′ and the trifluoromethyl ketone inhibitor. In all cases the charged surface residue is closer to the histidine than to the oxyanion. The interaction

Table IV: Comparison of Measured and Calculated Interaction Energies between Surface Charge at Positions 36 and 99 and His64 for Free Subtilisin BPN′

	Asp → Gln36		Asp → Ser99		Asp → Lys99	
ionic strength	calculated[a] (kcal mol^{-1})	measured (kcal mol^{-1})	calculated[a] (kcal mol^{-1})	measured[b] (kcal mol^{-1})	calculated[a] (kcal mol^{-1})	measured[b] (kcal mol^{-1})
0.01 M	0.32	0.25[c]	0.39	0.57	0.72	0.89
0.1 M	0.25		0.26	0.37	0.44	0.63
1.0 M	0.20	−0.01	0.11	0.07	0.15	0.25

[a] Calculated using the DelPhi software package. [b] Measured in phosphate buffer, with ionic strength adjusted by addition of KCl (Thomas *et al.*, 1985; Russell & Fersht, 1987; Russell *et al.*, 1987).

Table V: Interaction Energies between Surface Charges at Positions 36 and 99, and His64, and Oxyanion, Calculated Using DelPhi Using a Model of the Complex Formed between Subtilisin BPN′ and the Trifluoromethyl Ketone

	interaction energies (kcal mol^{-1})[a]											
	Asp → Gln36[b]				Asp → Ser99[b]				Asp → Lys99[c]			
ionic strength	$\Delta\Delta G_{+/0}$	$\Delta\Delta G_{0/-}$	$\Delta\Delta G_{+/-}$	[d]$\Delta\Delta G_{binding}$ measured	$\Delta\Delta G_{+/0}$	$\Delta\Delta G_{0/-}$	$\Delta\Delta G_{+/-}$	$\Delta\Delta G_{binding}$ measured[d]	$\Delta\Delta G_{+/0}$	$\Delta\Delta G_{0/-}$	$\Delta\Delta G_{+/-}$	$\Delta\Delta G_{binding}$ measured[d]
0.01 M	0.48	−0.15	0.33	0.10 ± 0.09	0.45	−0.24	0.21	0.15 ± 0.05	0.71	−0.49	0.22	0.46 ± 0.04
0.1 M	0.41	−0.10	0.31	0.20 ± 0.05	0.35	−0.14	0.21	0.20 ± 0.05	0.49	−0.26	0.23	0.58 ± 0.04
1.1 M	0.35	−0.06	0.29	−0.01 ± 0.08	0.24	−0.05	0.19	0.10 ± 0.07	0.27	−0.07	0.20	0.32 ± 0.04

[a] Calculated using DelPhi software package on a model of the subtilisin BPN′–trifluoromethyl ketone inhibitor complex based on the crystal structure of subtilisin BPN′–chymotrypsin inhibitor 2 complex (McPhalen & James, 1985). Default settings in version 2.3 were used. [b] Wild-type structure was used with aspartic acid residues at positions 36 and 99. [c] Lysine was modeled in an extended conformation into the structure at position 99 using the program FRODO (Jones, 1978). [d] Calculated from experimentally determined dissociation constants.

energy between the surface charge and the histidine is therefore greater than between the surface charge and the oxyanion. This is reflected in the values of $\Delta\Delta G_{+/-}$, which are positive.

DISCUSSION

Contribution of Long-Range Electrostatic Interactions to $\Delta\Delta G_{binding}$. Previous studies have looked at the effect of long-range electrostatic interactions on the ground state of enzymes (Thomas et al., 1985; Russell & Fersht, 1987; Russell et al., 1987; Cederholm et al., 1991). In this study, we have measured the effect of long-range electrostatic interactions on the transition state of an enzyme. Measurement of K_i for the complex between the trifluoromethyl ketone and wild-type and mutant subtilisins has been used to investigate the effect of long-range electrostatics on the stability of the complex and thus, by analogy, on the transition state of hydrolysis for subtilisin BPN′.

The experimental results clearly show that there is a small, but significant contribution to the binding energy from distant surface charges (Table III). The values of $\Delta\Delta G_{binding}$ are positive, indicating that increasing the positive charge on the surface of the enzyme destabilizes the transition-state complex. Theoretical calculations, using the DelPhi program, on a model structure representing the transition-state complex also show that long-range electrostatic interactions can stabilize or destabilize such a state depending upon the charge distribution (Table V). These results suggest that long-range electrostatic interactions will also be important in stabilizing the catalytic transition state of the enzyme.

Validity of the Method. There are a number of assumptions made in the method of analysis used. First, it is assumed that there are no structural rearrangements on mutation. Charged residues on the surface of the enzyme, which are not directly involved either in substrate binding or in the catalytic mechanism, were mutated. Such mutations were chosen to ensure that the only changes are electrostatic in nature. All the substitutions made were known to occur naturally in subtilisins from other species of *bacilli*. Such mutations are expected to have little or no effect on the conformation of the enzyme. Secondly, the complex formed between the trifluoromethyl ketone and subtilisin BPN′ is a reasonable model

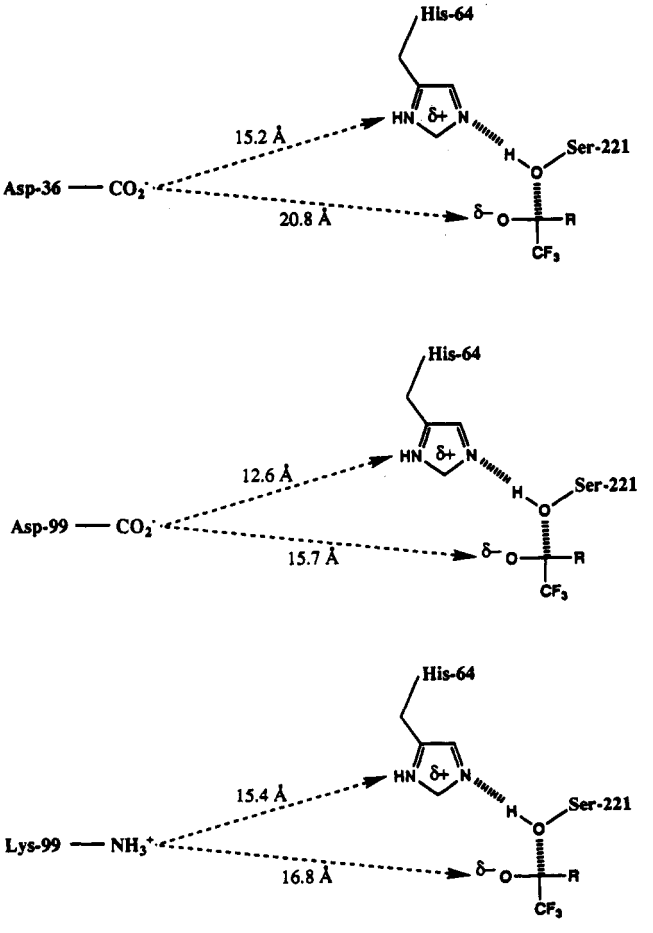

FIGURE 3: Stereochemical relationship between the surface charges on Asp36, Asp99, and Lys99 and the possible charges in the enzyme–transition state inhibitor complex.

of the transition state for hydrolysis of the enzyme. There is substantial evidence from other studies that the trifluoromethyl ketone–serine protease complex is a model for the transition state of catalysis of serine proteases and it is expected to be an accurate mimic of the tetrahedral intermediate. In particular, linear free energy relationships have been found

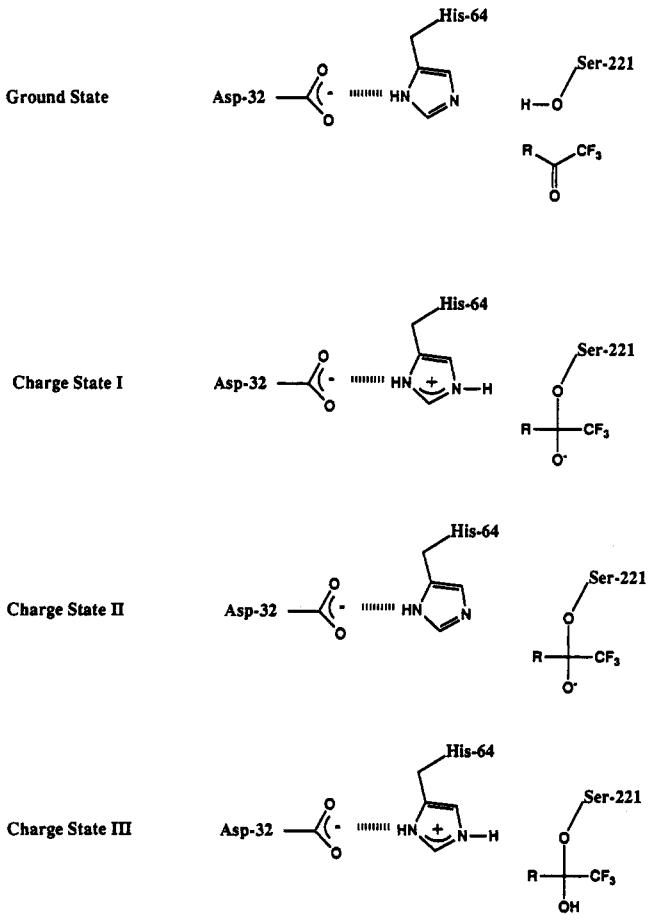

FIGURE 4: Possible charge distributions in the complex formed between subtilisin and Z-Ala-Ala-Pro-Phe-trifluoromethyl ketone.

between K_i and k_{cat}/K_m for the hydrolysis of corresponding substrates for several serine proteases, for example, chymotrypsin and porcine pancreatic elastase (Imperiali & Abeles, 1986) and human leukocyte elastase (Stein et al., 1987). Bartlett and Marlowe (1983) and Thompson (1973) have both pointed out that K_i for a series of transition-state analogues can be related to k_{cat}/K_m for the corresponding substrates. By analogy, we assume that a similar complex is formed between subtilisin BPN′ and the trifluroromethyl ketone.

Comparison of $\Delta\Delta G_{binding}$ Determined Experimentally and from Theoretical Calculations. By comparing the value of $\Delta\Delta G_{binding}$ determined experimentally and from theoretical calculations, it is possible to use long-range electrostatic interactions to probe the charge distribution within the transition-state complex. The possible charge distributions both in the complex and in the ground state of the enzyme have to be taken into account in the theoretical calculation of the electrostatic contribution to the binding energy. The ground state of the enzyme, as well as three possible charge distributions in the complex, is shown in Figure 4. In the ground state the active site aspartic acid is ionized and makes a hydrogen bond with the active site histidine.

In charge state III, the aspartic acid remains ionized, the histidine is protonated and therefore charged, but the oxyanion is not ionized. In this case, $\Delta\Delta G_{calc}$ is given by $\Delta\Delta G_{+/0}$ in Table V. All mutations would have a destabilizing effect on the stability of the complex, with $\Delta\Delta G_{calc}$ in the order of 0.45–0.71 kcal mol^{-1}, at low ionic strength. Experimentally determined values for $\Delta\Delta G_{binding}$ show that although the effects of the mutations are destabilizing, the magnitudes of the changes are much less than predicted for such a charge distribution.

In charge state II, the aspartic acid is ionized, the histidine is unprotonated and uncharged, and the oxyanion is ionized. In this case, $\Delta\Delta G_{calc}$ is given by $\Delta\Delta G_{0/-}$ in Table V, and all mutations would be stabilizing. This is not observed experimentally.

In charge state I, the aspartic acid remains ionized, the histidine is protonated and carries a positive charge, and the oxyanion is ionized. In this case, $\Delta\Delta G_{calc}$ is given by $\Delta\Delta G_{+/-}$ (Table V). All mutations would result in a net destabilization of the complex; however, since $\Delta\Delta G_{+/0}$ and $\Delta\Delta G_{0/-}$ are of opposite sign, the overall changes would not be large. Predicted values range between 0.21 and 0.33 kcal mol^{-1}, at low ionic strength. There is an excellent agreement between the results obtained experimentally for the Asp → Ser99 mutation and those calculated theoretically for this charge distribution. The other two mutations, Asp → Gln36 and Asp → Lys99, however, are not modeled so well. In the case of Asp → Lys99 the values obtained experimentally are somewhat higher than those predicted. This may result from modeling the lysine residue in the structure of the complex in a single conformation. Surface lysines such as this are usually ill-defined in crystal structures as they frequently adopt more than one conformation. The values obtained experimentally for Asp → Gln36 are slightly lower than those predicted; however, the errors involved in the measurement of this mutant are somewhat higher than the others. The value at 0.1 M Tris-HCl, determined with the lowest error, is in reasonable agreement with $\Delta\Delta G_{+/-}$. Although the results are not sufficiently accurate to be able to distinguish clearly between the different charge distributions within the complex, the results are most consistent with a transition state in which an ion pair is formed between the histidine and the oxyanion (Table V).

There is substantial evidence from studies on other serine proteases that both histidine and oxyanion are charged in the complex. The pK_as of the histidine and the oxyanion have been measured for complexes of peptidyl trifluoromethyl ketones and acetylcholinesterase (Allen & Abeles, 1989), and chymotrypsin (Liang & Abeles, 1987; Brady et al., 1989). In both of these studies the pK_a of the active site histidine is estimated to be below 4, and the pK_a of the oxyanion is found to be over 10, in the complex. Assuming that similar pK_a shifts occur in the complex with subtilisin BPN′, at pH 8.6 both the histidine and the oxyanion would carry full charges, consistent with experimental and theoretical results.

Comparison of the Theoretical Calculations of the Long-Range Electrostatic Interactions between Free and Complexed Enzyme. The DelPhi software package was used to calculate the magnitude of electrostatic interactions between a distant surface charge, at position 36 or 99, and the active site histidine in both free enzyme and in a model complex. The results are shown in Tables IV and V respectively. In all cases the results show that the magnitude of the electrostatic interactions are larger in the complex than in the free enzyme. In the complex the active site is effectively desolvated by the presence of the bound inhibitor. This is also the case for the transition state in which substrate is bound. His64 is, therefore, buried and no longer accessible to solvent. Thus, the "local" dielectric constant is much lower than it would be in the free enzyme, and the electrostatic interaction energies are, therefore, larger. As a consequence, long-range electrostatic interactions maybe more important in the transition state of an enzyme than in the ground state because of the effect of desolvation.

The exclusion of water from the active site of the complex also affects the screening of long-range electrostatic interactions by salt. The electrostatic interactions in the complex (Table V) are screened less by salt than in the free enzyme

(Table IV). This results from the fact that sodium and chloride ions can no longer penetrate into the active site because of the presence of the bound inhibitor. The screening of the electrostatic interaction between the charge at position 36 or 99, and His64 and the oxyanion, is very similar. Thus, the overall interaction energy, $\Delta G_{+/-}$, is hardly affected by salt (Table V). This is also observed experimentally (Table III). This is in comparison to the results found both experimentally and theoretically for the free enzyme in which there is a significant decrease in the electrostatic energy with increasing ionic strength.

CONCLUSIONS

We have shown not only that long-range electrostatic interactions can be used to probe the charge distribution in a transition-state complex but also that these long-range electrostatic interactions can affect the stability of such a state. We have shown this both experimentally, using measured values of K_i for the complex formed between a trifluoromethyl ketone and wild-type and mutant subtilisins, and theoretically, using the DelPhi software package.

For the complex formed between the trifluoromethyl ketone and subtilisin BPN′, the experimental results are found to be most consistent with a charge distribution in which an ion pair is formed between the active site histidine and the ionized oxyanion. Long-range electrostatic interactions are found to affect the stability of the transition-state complex by up to 0.6 kcal mol^{-1}. This suggests that long-range electrostatic interactions also play a role in stabilizing catalytic transition states. This kind of transition-state stabilization maybe very important for enzymes which have a very asymmetric distribution of surface charge.

ACKNOWLEDGMENT

We thank Professor Robert H. Abeles for the generous gift of Z-Ala-Ala-Pro-Phe-trifluoromethyl ketone.

REFERENCES

Allen, K. N., & Abeles, R. H. (1989) *Biochemistry 28*, 8466–8473.

Angliker, H., Wikstrom, P., Rauber, P., Stone, S., & Shaw, E. (1988) *Biochem. J. 256*, 481–486.

Bartlett, P. A., & Marlowe, C. (1983) *Biochemistry 22*, 4618–4624.

Bash, P. A., Field, M. J., Davenport, R. C., Petsko, G. A., Ringe, D., & Karplus, M. (1991) *Biochemistry 30*, 5826–5832.

Bender, M. L., Begue-Canton, M. L., Blakeley, R. L., Brubacher, L. J., Feder, J., Gunter, C. R., Kezdy, F. J., Killheffer, J. V., Marshall, T. H., Miller, C. G., Roeske, R. W., & Stoops, J. K. (1966) *J. Am. Chem. Soc. 24*, 5890–5913.

Bott, R., Ultsch, M., Kossiakoff, A., Graycar, T., Katz, B., & Power, S. (1988) *J. Biol. Chem. 263*, 7895–7906.

Brady, K., Liang, T.-C., & Abeles, R. H. (1989) *Biochemistry 28*, 9066–9070.

Bryan, P., Pantoliano, M. W., Quill, S. G., Hsiao, H.-Y., & Poulos, T. (1986) *Proc. Natl. Acad. Sci. U.S.A. 83*, 3743–3745.

Cederholm, M. T., Stuckey, J. A., Doscher, M. S., & Lee, A. (1991) *Proc. Natl. Acad. Sci. U.S.A. 88*, 8116–8120.

Cha, S. (1975) *Biochem. Pharmacol. 24*, 2177–2185.

Dao-Pin, S., Liao, D.-I., & Remington, S. J. (1989) *Proc. Natl. Acad. Sci. U.S.A. 86*, 5361–5365.

DelMar, E. G., Largman, C., Broderick, J. W., & Geokas, M. C. (1979) *Anal. Biochem. 99*, 316–320.

Dunlap, R. P., Stone, P. J., & Abeles, R. H. (1987) *Biochem. Biophys. Res. Commun. 145*, 509–513.

Gilson, M., Rashin, A. A., Fine, R., & Honig, B. H. (1985) *J. Mol. Biol. 184*, 503–516.

Gilson, M., Sharp, K., & Honig, B. (1988) *J. Comput. Chem. 9*, 327–335.

Govardhan, C., & Abeles, R. H. (1990) *Arch. Biochem. Biophys. 280*, 137–146.

Imperiali, B., & Abeles, R. H. (1986) *Biochemistry 25*, 3760–3767.

Imperiali, B., & Abeles, R. H. (1987) *Biochemistry 26*, 4474–4477.

Kettner, C. A., & Shenvi, A. B. (1984) *J. Biol. Chem. 259*, 15106–15114.

Klapper, I., Hagstrom, R., Fine, R., Sharp, K., & Honig, B. (1986) *Proteins: Struct., Funct., Genet. 1*, 47–59.

Koppenol, W. (1981) *Oxygen and Oxy-Radicals in Chemistry and Biology* (Rogers, M., & Powers, E., Eds.) pp 674–691, Academic Press, New York.

Koppenol, W., & Margoliash, E. (1982) *J. Biol. Chem. 257*, 4426–4437.

Liang, T.-C., & Abeles, R. H. (1987) *Biochemistry 26*, 7603–7608.

Loewenthal, R., Sancho, J., Reinikainen, T., & Fersht, A. R. (1993) *J. Mol. Biol. 232*, 574–583.

Matsubara, H., Kaspar, C. B., Brown, D. M., & Smith, E. L. (1965) *J. Biol. Chem. 240*, 1125–1130.

Matthew, J. B., Hanania, G. I. H., & Gurd, F. R. N. (1979) *Biochemistry 18*, 1919–1928.

McMurray, J. S., & Dyckes, D. F. (1986) *Biochemistry 25*, 2298–2301.

McPhalen, C. A., Svendsen, I., Jonassen, I., & James, M. N. G. (1985) *Proc. Natl. Acad. Sci. U.S.A. 82*, 7242–7246.

Northrup, S., Boles, J., & Reynolds, J. (1988) *Science 241*, 67–70.

Perry, K. M., Onuffer, J. J., Gittelman, M. S., Barmat, L., & Matthews, C. R. (1989) *Biochemistry 28*, 7961–7968.

Perutz, M. (1978) *Science 201*, 1187–1191.

Pickersgill, R. W., Goodenough, P. W., Sumner, I. G., & Collins, M. E. (1988) *Biochem. J. 254*, 235–238.

Ritchie, C. D. (1984) *J. Am. Chem. Soc. 106*, 7187–7194.

Robertus, J. D., Kraut, J., Alden, R. A., & Birktoft, J. J. (1972) *Biochemistry 11*, 4293–4303.

Russell, A. J., & Fersht, A. R. (1987) *Nature 328*, 496–500.

Russell, A. J., Thomas, P. G., & Fersht, A. R. (1987) *J. Mol. Biol. 193*, 803–813.

Smith, R. A., Copp, L. J., Donnelly, S. L., Spencer, R. W., & Krantz, A. (1988) *Biochemistry 27*, 6568–6573.

Soman, K., Yang, A.-S., Honig, B., & Fletterick, R. (1989) *Biochemistry 28*, 9918–9926.

Stein, R. L., & Strimpler, A. M. (1987) *Biochemistry 26*, 2611–2615.

Stein, R. L., Strimpler, A. M., Edwards, P. D., Lewis, J. J., Mauger, R. C., Schwartz, J. A., Stein, M. M., Trainor, D. A., Wildonger, R. A., & Zottola, M. A. (1987) *Biochemistry 26*, 2682–2689.

Takahashi, L. H., Radhakrishnan, R., Rosenfield, R. E., Jr., & Meyer, E. F., Jr. (1989) *J. Mol. Biol 201*, 423–428.

Thomas, P. G., Russell, A. J., & Fersht, A. R. (1985) *Nature 318*, 375–376.

Thompson, R. C. (1973) *Biochemistry 12*, 47–51.

Tweedy, N. B., Hurle, M. R., Chrunyk, B. A., & Matthews, C. R. (1990) *Biochemistry, 29*, 1539–1545.

Warshel, A. (1981) *Acc. Chem. Res. 14*, 284–290.

Warshel, A., Russell, S. T., & Churg,, A. K. (1984) *Proc. Natl. Acad. Sci. U.S.A. 81*, 4785–4789.

Warwicker, J., & Watson, H. C. (1982) *J. Mol. Biol. 157*, 671–679.

Williams, J. W., & Morrison, J. F. (1979) *Methods Enzymol. 63*, 437–467.